Splash of a drop impacting onto a solid substrate wetted by a thin film of another liquid

Hannah M. Kittel, Ilia V. Roisman,[*] and Cameron Tropea
Technische Universität Darmstadt, Germany Institute of Fluid Mechanics and Aerodynamics,
Alarich-Weiss-Straße 10, 64287 Darmstadt, Germany

In this study, the impact of a liquid drop onto a thin liquid film of a different fluid is investigated experimentally using a high-speed video system and analysed theoretically to obtain expressions for predicting splashing thresholds. The study focuses on impact conditions leading to one of four outcomes: deposition, corona without splash, corona splash, and partial rebound. In addition to the conventional influencing parameters, which are usually described by combinations of impact Weber and Reynolds numbers and dimensionless film thickness, also the ratio of the drop and film liquid viscosities have been systematically varied over a wide range. The results of the theoretical analysis, in good agreement with the experimental observations, show that the well-known K number determines the splashing threshold only if the viscosity of the film is much larger or much smaller than the drop viscosity. If the drop and film viscosities are comparable, a critical modified K number is introduced, which is a function of the viscosity ratio.

I. INTRODUCTION

The impact of a drop onto a surface, whether it is dry or wetted, soft or solid, has been extensively investigated in the past. Prediction of splashing as a result of drop impact onto a wetted substrate is rather important for modeling of different industrial processes, like spray coating or painting [1–5], microencapsulation [6,7], spray cooling [8,9], and internal engine combustion [10,11]. For example, fuel mixture preparation in modern combustion engines is influenced by the interaction of fuel spray droplets impacting onto lubricating oil films on the cylinder walls, resulting in splashing of mixed component drops into the combustion chamber. Another example is the injection of AdBlue into the exhaust gas system of a vehicle. AdBlue is an aqueous urea solution of 32.5 wt.% urea, which is injected into the selective catalytic reduction in order to improve the emissions of a diesel engine. The effect of AdBlue injection is influenced, among other parameters, by the content of the urea/water film already existing on the wall, since this influences the composition of the splashed droplets. Besides applications in the automotive industry, spray cooling during the process of forming and forging and the role of additives in the lubrication solvents are further examples of where information regarding the splash occurrence after drop impact is of importance. The drop/wall interaction in all of these cases is affected by the fact that the drop and the liquid film are different liquids and may exhibit different degrees of miscibility.

Drop impact onto a wetted wall results in several different impact outcomes dependent on the impact parameters [12]. Drop impact can lead to phenomena like deposition or drop rebound, corona or prompt splash, and jetting or local dewetting [13–15]. The drop initially penetrates the wall liquid film, creating a crater. This crater first expands and then retracts because of capillary forces and
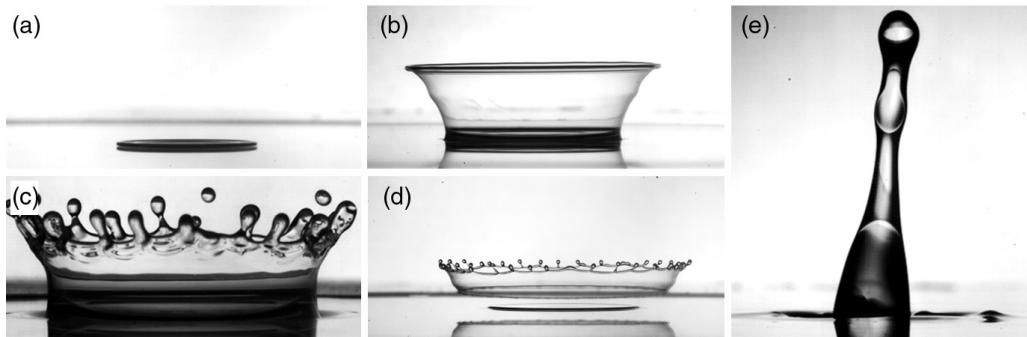
---

[*]roisman@sla.tu-darmstadt.de

FIG. 1. Different impact outcomes: (a) deposition, (b) corona (without splash), (c) corona splash, (d) corona detachment, and (e) partial rebound.

gravity. If the impact velocity of the drop is relatively low, the impact generates a set of circular waves expanding on the wall film. At higher impact velocity and surface tension, retraction of the crater can lead to the generation of a central jet. In some cases, this jet breaks up, leading to partial drop rebound.

One of the most important outcomes for many technical applications is splashing, occurring when drop impact leads to the generation of a number of secondary droplets. Two main kinds of splash have been identified, the corona splash and the prompt splash. In *prompt splash,* fine secondary droplets are produced from the jets ejected immediately after the impact.

The *corona splash* occurs when the inertial effects in the flow generated by drop impact are significant. The formation and expansion of the corona is explained in Ref. [16] by the kinematic discontinuity of the wall film. This inviscid theory [16,17], valid for very high Reynolds and Weber numbers of impact, allows prediction of the temporal evolution of the corona radius (at the base of the corona) as $R_{\mathrm{corona}} \sim t^{1/2}$. At large times of corona expansion, the influence of surface tension becomes significant. These forces, together with gravity, lead to deviation of the radius expansion from the square root dependence on time predicted by inviscid theory. Moreover, at some instant the radius reaches a maximum and the crater begins to recede. These phenomena are investigated in detail and modeled in Refs. [18,19].

The effect of capillary forces is also significant at the edge of the uprising sheet forming the corona. These forces lead to the formation of a propagating rim [16,20,21], growing due to the flow entering the rim from the free liquid sheet. A rim bounding an uprising sheet is unstable. If the corona expansion time is long enough, the rim instability can lead to the formation of cusps [13,16] and finger-like jets, which then finally break up and generate a number of secondary droplets (*corona splash*), as shown in Fig. 1(c).

The outcome of drop impact is influenced by the impact parameters (drop diameter D_0 and impact velocity U_0) and the material properties of the fluids (kinematic viscosity ν, density ρ, and surface tension σ). Correspondingly, the main dimensionless parameters describing drop impact are the Reynolds and Weber numbers, defined as

$$\mathrm{Re} = \frac{D_0 U_0}{\nu}, \quad \mathrm{We} = \frac{\rho D_0 U_0^2}{\sigma}, \tag{1}$$

respectively.

The splashing threshold for drop impact onto a wetted substrate has been introduced in the form of the critical K number [22], defined as

$$K = \mathrm{We}^{1/2}\mathrm{Re}^{1/4}. \tag{2}$$

The formulation of the parameter K can be explained by the assumption that splash occurs when the inertial forces are much larger than forces associated with surface tension [16,23]. An empirical
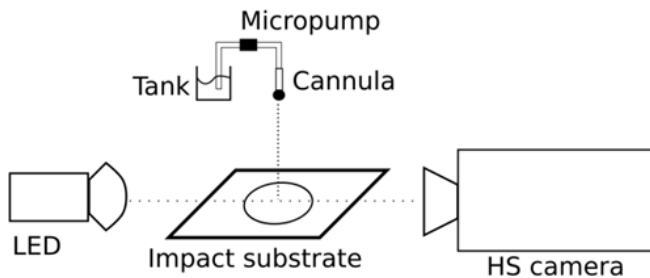
FIG. 2. Schematic illustration of the experimental setup.

expression for the critical K number [23] for drop impact onto a film is

$$K_{\text{critical}}^{8/5} = 2100 + 5880\delta^{1.44}, \quad \delta = \frac{h}{D_0}, \tag{3}$$

where h is initial thickness of the unperturbed film and δ is its dimensionless value.

More recent studies [24] on drop impact onto thin liquid films ($\delta < 0.15$) claim that the K number is still not a reliable dimensionless parameter. Moreover, the K number is definitely not suitable for the description of drop impact onto dry solid substrates [25].

The splashing threshold of a drop impacting onto a thin film [26] is obtained in the form

$$(\text{Re}^{0.17}\text{We}^{0.5})_{|\text{critical}} = 63; \tag{4}$$

however, the relative film thickness δ has not been documented in these experiments.

The splashing threshold in the case of inclined drop impact onto a deep pool [27] is described by the critical K number computed using the normal component of the impact velocity. The corresponding splashing threshold is

$$K_{\text{n,critical}}^{8/5} \approx 2100, \quad \delta \gg 1. \tag{5}$$

In most of the previous studies, the impact of a liquid drop onto a substrate wetted by the same liquid has been considered. Only very few authors have investigated the impact onto a wall wetted by another liquid experimentally [28–30] or numerically [31]. A reliable model able to predict the outcome of drop impact in the case when the drop and wall film are different liquids has not yet been developed.

The main subject of the present study is the experimental investigation of a single drop impact onto a horizontal liquid film of a different liquid. The influencing factors of the impact outcome, and in particular of the splashing threshold, are investigated. The splashing threshold has been determined for various ratios of the liquid viscosities and impact parameters. In this study, only thin films with a small relative film thickness of $\delta \leqslant 0.3$ are investigated and the liquids used are Newtonian.

For certain impact conditions, other types of outcomes have been identified. Among them is corona detachment from the liquid film [32]. However, in this study only cases leading to drop deposition (without generation of secondary drops) or splash caused by breakup of the rim bounding a corona are considered. All other cases are excluded from the discussion of the results as they are only found for special conditions and involve different physical mechanisms of splash.

II. MATERIALS AND METHODS

The experimental setup is shown schematically in Fig. 2. The setup consists of three main systems: the liquid supply and drop generator, the substrate with the wall film, and the observation system. In this study, both liquids of the drop and the wall film are Newtonian. Table I summarizes the physical properties of the fluids used.

TABLE I. Material properties (kinematic viscosity ν, surface tension σ, and density ρ) of the liquids used in this study: distilled water, hexadecane, and various types of silicon oil of different viscosities.

	ν [mm^2/s]	σ [mN/m]	ρ [kg/m^3]
Water	1.004	72.24	997
Hexadecane	4.11	27.61	769.15
S5	5	17.72	910
S10	10	18.19	930
S20	20	18.2	945
S25	25	18.19	950
S50	50	18.69	960
S65	65	18.2	970
S350	350	18.56	972
S500	500	18.83	972
S750	750	18.6	972
S1000	1 000	18.59	972
S10000	10 000	18.81	972
S30000	30 000	18.81	972
S100000	100 000	18.81	972

The drop generator is based on the drop-on-demand method. A micropump transports the fluid from a tank to the cannula on demand. The fluid forms a drop at the tip of the cannula due to its surface tension until finally a critical mass is reached. Then the drop drips off the cannula tip driven by gravity. Using different tip diameters of the cannula, the drop diameter can be varied. In this study, three cannulas are used with the tip diameters 0.3, 0.6, and 0.8 mm. Correspondingly, with these cannulas water drops of diameters $D_0 = 2.1$, 2.6, and 2.8 mm are formed. The diameters of the silicon oil drops are 1.8, 2, and 2.2 mm for all the oil types used. The impact velocity of the drop is determined by the distance of the cannula tip above the fluid interface and the gravitational acceleration. In this study, the impact velocity U_0, estimated from the analysis of the captured high-speed videos of a falling drop, varies from 1.7 to 3.2 m/s.

A horizontal glass plate is used as an impact substrate. The glass plate is sandblasted up to a recessed edge onto which a vertical metal plate was exactly fitted and glued. The diameter of the ring is set to 60 mm in order to avoid edge effects. In this manner, a wall film of defined thickness could be realized. In order to study the effect of the film thickness ratio on drop impact outcome, three different wall film thicknesses h were used in this study: 0.1, 0.25, and 0.5 mm.

The wall film thickness is measured using a micrometer screw. First, the dry tip of the micrometer screw is dropped until it touches the liquid surface of the wall film. Afterward, the screw is dropped until it touches the glass substrate. The film thickness is determined by the difference of both values. The estimated error of the film thickness measurement is 2%.

The observation system consists of a high-speed video camera and an illumination source. The impact substrate is located between the camera and the illumination source. In front of the illumination source, a diffusing screen is placed in order to achieve a uniform background lighting. The frame rate of the high-speed video camera (Photron Fastcam SA-X2) can been chosen up to 40 000 fps with a resolution of 576×480 pixels and a shutter time of 10 μs. The illumination source is a light-emitting diode (LED, Veritas Constellation 120E, 12 000 lm).

Using the observation system, the impact phenomenon is captured, the impact outcome is determined, and among other quantities, the crown height and its diameter are determined as a function of time. In the study, the drop diameter, the impact velocity, the film thickness, and the fluid properties of the drop and wall film are varied.
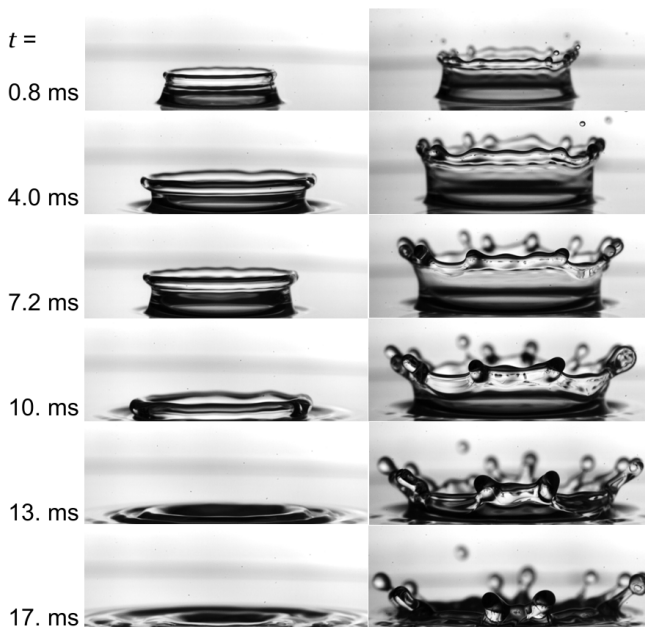
FIG. 3. Drop size influence on corona development: S65 drop impacting onto a water film with $\kappa = 0.015$, $U_0 = 2.3$ m/s, and $h = 0.5$ mm. Drop diameter is $D_0 = 1.8$ mm (left) and 2.2 mm (right), resulting in dimensionless film thicknesses of $\delta = 0.28$ and 0.23.

III. EXPERIMENTAL OBSERVATIONS

In this study, four different impact outcomes have been observed: deposition, corona (without splash), corona splash, and partial rebound. In order to understand the dynamics of drop impact and to be able to develop a theoretical model predicting the impact outcome, the influencing parameters have to be identified and their effects have to be determined. In the present case, these parameters encompass the impact drop diameter D_0 and velocity U_0, as well as the fluid properties of the two fluids being used—drop and wall film—in particular, the kinematic viscosity ν. In order to describe the fluid combination, the viscosity ratio is used and defined as $\kappa = \nu_f / \nu_d$. To begin, the influence of each parameter is considered separately in a series of visualizations.

The influence of the drop diameter on the impact outcome is shown in Fig. 3. A larger drop enhances splashing. As shown in Fig. 4, the impact velocity also enhances splashing. The influence of the film thickness on the impact outcome in the regime of thin films ($\delta < 1$) is not as clear. As can be seen in Fig. 5, the impact outcome is comparable for different film thicknesses. Also, the differences in the corona diameters and heights are minor. In Ref. [33], the angle β of the corona inclination to the target plane is predicted in the form

$$\cos \beta = 1 - 4\delta. \tag{6}$$

However, in this study the observed angle of the corona inclination is about $\beta \approx 80°$ for all three film thicknesses during corona propagation ($t = 2$–5 ms), which differs significantly from the prediction given in Eq. (6).

If different fluids are used for the drop and wall film, then one can expect that the properties of both fluids must be considered when discussing their influence on the outcome. However, not only the fluid properties are important, but also which liquid is used for the drop or wall film, as can be seen in Fig. 6. The impact outcome as well as the temporal evolution of the corona are strongly determined by which liquid is used for the drop and which for the wall film. With increasing viscosity
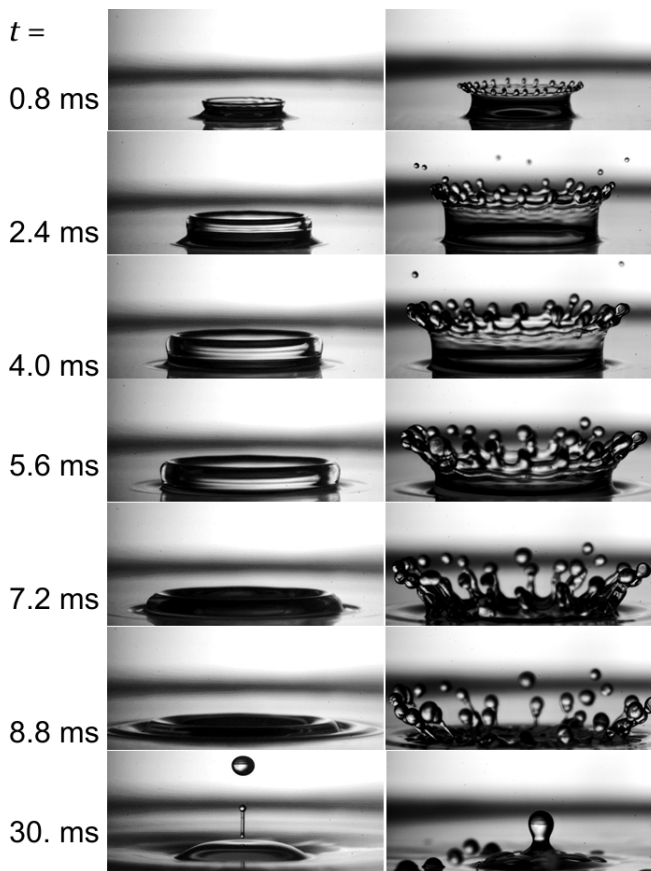
FIG. 4. Impact velocity influence on corona development: water drop ($D_0 = 2$ mm) impacting onto a S10 film with $h = 0.5$ mm and $\kappa = 9.9$. Impact velocity is $U_0 = 1.7$ (left) and 2.3 m/s (right).

of the wall film, the corona evolution becomes slower due to the increasing resistance force of the wall liquid. Conversely, a less viscous wall film yields more easily and promotes the evolution of the corona. Therefore, corona splash occurs more readily in the case of a less viscous wall film. The influence of the drop viscosity is not as obvious.

Comparing the outcomes of the same drop impacting onto different wall film liquids, as can be seen in Fig. 7, the outcome does not differ significantly. In this figure, impact onto glass is also pictured for comparison. The impact onto a high-viscosity wall film does not differ significantly from impact onto glass, as would be expected. The impact surface strongly determines the behavior of the drop after impact, i.e., whether the drop can build a corona or whether the fluid of the drop is arrested and ends in deposition. Directly after the impact, a very high-viscosity drop simply sits on the impact substrate but does not spread. For such high-viscosity drops, two spreading phases can be observed (Fig. 7). In the first phase, lasting a couple of milliseconds, the drop is only deformed breadthwise and then the motion of the drop is stopped. No spreading lamella is observed. In the second phase, which lasts several seconds, the contact angle slowly decreases.

If the liquid of the wall film is less viscous, the impact leads to the evolution of a corona. Furthermore, it can also lead to corona splash, depending on the properties of the wall film. Whereas the impact outcome is influenced strongly by the viscosity of the wall film, the maximum spreading diameter $D_{\max}$ and maximum corona diameter $D_{cr,\max}$ are more strongly influenced by the viscosity of the drop, as can be observed in the case of deposition discussed above. With increasing viscosity
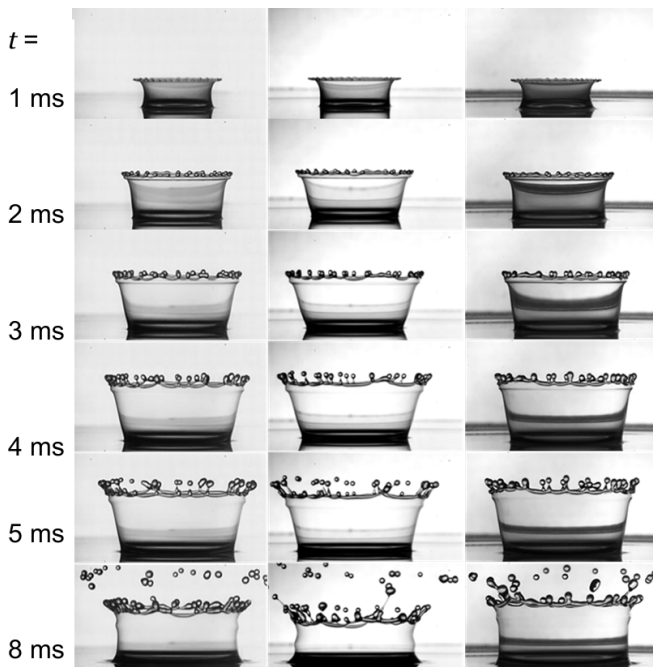
FIG. 5. Film thickness influence on the corona development: A S5 drop impacting onto a S10 wall film with from left to right $\delta = 0.04$, 0.11, and 0.23. The impact velocity is $U_0 = 3.2$ m/s, the drop diameter is $D_0 = 2.2$ mm, and the viscosity ratio is $\kappa = 0.5$. Relevant movies can be found at Ref. [34].

of the drop, $D_{cr,\max}$ decreases, whereas an increase of the wall film viscosity does not significantly influence $D_{cr,\max}$, as shown in Fig. 8.

It appears that the fluid of the drop is the dominating factor determining the impact outcome (deposition, corona with splash, corona splash, partial rebound). The fluid of the wall film is more influential in determining the splashing threshold, as can be seen in Fig. 8. In the case of a highly viscous drop, the splashing threshold is already reached at a wall film viscosity of $\nu_f = 20$ mm^2/s.

Nevertheless, the wall film can also influence the impact outcome. For a highly viscous wall film, the drop cannot evolve to a corona since the resistance of the wall film is too high and does not permit the evolution of a spreading lamella and subsequent corona. The drop barely penetrates or deforms the wall film; thus, the drop spreads like on a solid surface. If the wall film is less viscous, the impact leads to a corona or even to corona splash. In both cases, the maximum spreading diameter and the maximum corona diameter vary, depending on the viscosity of the drop. Similar to a highly viscous wall film, a highly viscous drop does not change its shape too much.

Figure 9 shows the impact outcome for different viscosity ratios. It can be seen that the impact outcome differs for different viscosity ratios. However, no clear correlation between the viscosity ratio and the impact outcome can be discerned. Although the impact outcome is clearly influenced by the viscosity ratio, the viscosity ratio itself cannot be used to predict the impact outcome.

IV. DYNAMICS OF A DROP IMPACT ONTO A LIQUID LAYER

The previous section illustrates clearly that the outcome of drop impact onto a film of a different liquid depends not only on the impact parameters but also on the viscosities of the drop and film. It is very difficult to understand or analyze experimental data if so many parameters influence the problem. Therefore, some fundamental discussion about the dynamics of drop impact is necessary prior to any analysis of the experimental results.
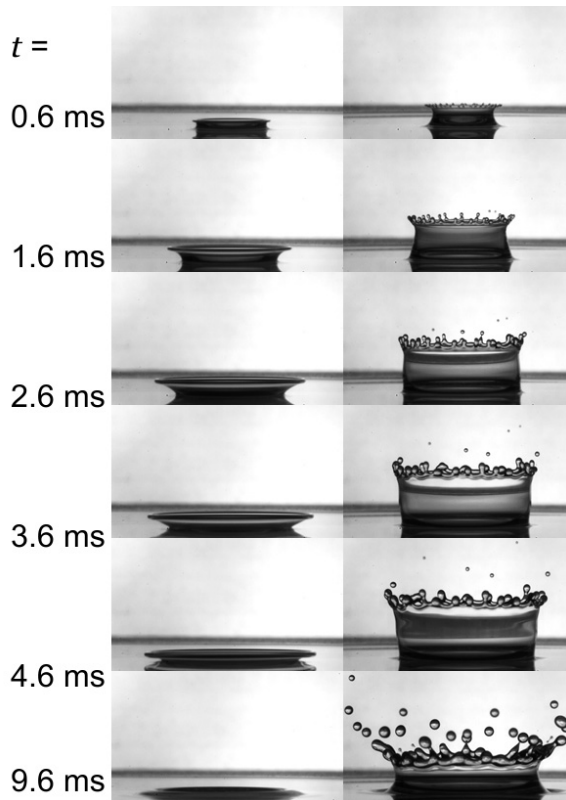
FIG. 6. Influence of fluid combination on the corona development: Impact of a S5 drop onto a S65 film (left) with $\kappa = 13$ and of a S65 drop impacting onto a S5 film (right) with $\kappa = 0.08$ for $\delta = 0.25$, $U_0 = 2.3$ m/s, and $D_0 = 2$ mm.

If the impact velocity is high enough, which means that both Reynolds and Weber numbers are much larger than the unity, the flow in the spreading lamella can be subdivided into an outer solution and the near-wall viscous boundary layer. In the outer solution, the influence of the viscous and capillary terms are negligibly small in comparison with the dominant inertial terms. This solution determines the flow in the lamella whenever the thickness of the viscous boundary layer is much smaller than the thickness of the lamella. At later stages, viscous terms become dominant. In the next sections, the main flow regions and impact phases are considered in more detail.

A. Inertia dominated flow in the spreading lamella: Outer solution

When a drop impacts onto a liquid layer, the dynamic pressure at the drop/film interface leads to the generation of a crater. The liquid layer between the expanding crater and the substrate consists of the two liquid films. The upper film corresponds to the drop liquid and the lower film corresponds to the liquid of the initial wall film. If the impact velocity is high enough, i.e., the impact Reynolds and Weber numbers are much larger than unity, then the flow in the radially expanding liquid layer is inertia dominated. The remote asymptotic solution for potential flow in the spreading lamella, valid for large times, has been obtained in Ref. [16] from the mass and momentum balance equations

$$u_r = \frac{r}{t + \tau D_0/U_0}, \quad u_z = -\frac{z}{2(t + \tau D_0/U_0)}, \quad (7)$$
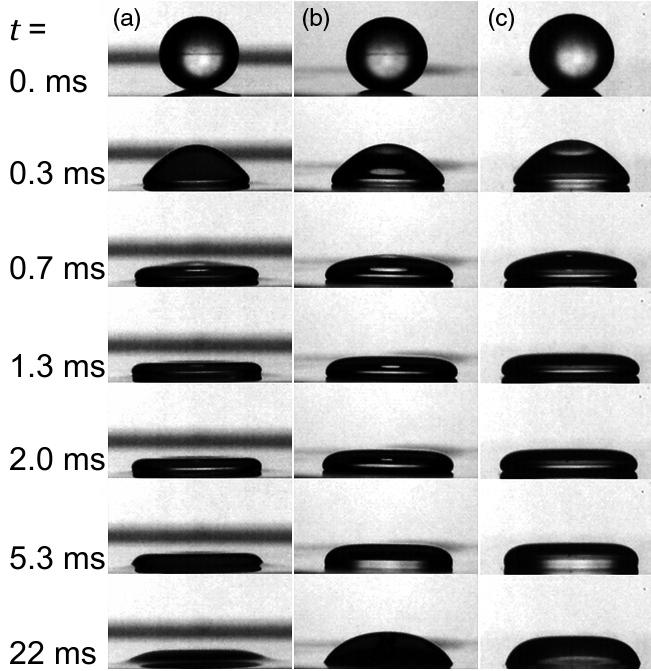
FIG. 7. Temporal development of the spreading of a S350 drop impacting onto wall films ($\delta = 0.23$) of different viscosities: (a) wall film of S1000; (b) wall film of S100000; and (c) impact onto glass for comparison. The impact velocity is $U_0 = 3.2$ m/s and drop diameter is $D_0 = 2.3$ mm.

where r and z are the radial and axial coordinates in the system with the origin fixed at the point of impact on the substrate, u_r and u_z are the radial and axial components of the velocity vector, and τ is a dimensionless constant, which depends only on the relative film thickness. The thickness of the lamella at large times is obtained in the form [16]

$$h_{\text{lam}} = \frac{\eta D_0^3}{U_0^2 (t + \tau D_0/U_0)^2},$$ (8)

where η is a dimensionless constant. This scaling has been confirmed by experiments on drop impact onto a spherical target [35].

The expanding film in the lamella interacts with the outer unperturbed liquid film. In Ref. [16], this interaction has been described as a propagation of a kinematic discontinuity, associated with the corona. The thickness of the sheet in the expanding corona is obtained from a mass balance of the kinematic discontinuity. This thickness is physically the sum of the thicknesses of the outer film and of the instantaneous thickness of the lamella in the crater region. The evolution of the corona radius is described using the mass and momentum balance equations and is expressed in the form

$$R_{\text{corona}} = \beta U_0^{1/2} D_0^{1/2} \left(t + \frac{\tau D_0}{U_0} \right)^{1/2},$$ (9)

where β is a dimensionless constant determined mainly by the dimensionless initial film thickness.

In Ref. [18], the expression for $R_{\text{corona}}(t)$ has been generalized by taking into account the effects associated with the surface tension and gravity. It is shown that the dimensionless maximum corona diameter, scaled by the drop diameter, is determined only by the impact Weber number and by the relative initial wall film thickness.
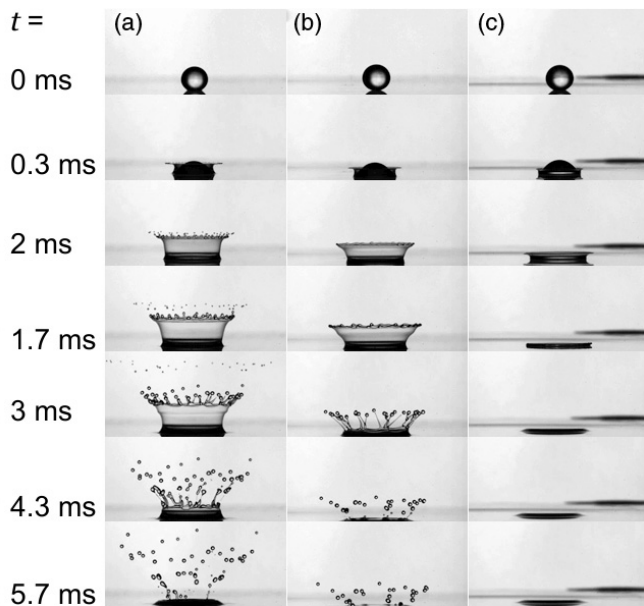
FIG. 8. Temporal development of the corona evolution of a S350 drop impacting onto different wall films: (a) S5; (b) S10; and (c) S20 for the same dimensionless film thickness $\delta = 0.04$, impact velocity of $U_0 = 3.2$ m/s, and drop diameter of $D_0 = 2.3$ mm.

B. Enigmatic viscosity effect on splash

Numerous experiments [18,19,36] demonstrate that if the Reynolds number is very high, the viscosity influence on the corona spreading is minor. On the other hand, the size of the secondary drops produced by splashing of an impacting spray on a wall, is scaled well by the size of the viscous boundary layer developing under the spreading lamella, which is expressed in Ref. [13] in the form

$$\frac{D_{\text{secondary}}}{D_{\text{primary}}} \sim \text{Re}^{-1/2}. \tag{10}$$

Moreover, the use of the K number, defined in Eq. (2), for quantifying the splash threshold is justified in Ref. [23], also using the concept of the viscous boundary layer. The effect of viscosity on the splashing threshold and on the mechanism of splash is thus unequivocal, if perhaps not very transparent. Why then does the viscosity not strongly affect corona spreading? This question will be addressed in the following with the aid of Fig. 10.

At the initial stage of corona expansion, the viscosity influences only the formation and growth of a viscous boundary layer near the substrate. When the thickness of the boundary layer is much smaller than the thickness of the spreading lamella, the influence of the viscosity on the kinematics of drop impact and corona expansion is minor. This situation is the same for the case of drop impact onto a dry substrate (considered in Refs. [37,38]) and a wetted substrate, as shown schematically in Fig. 10.

Let us assume that splash occurs when inertial effects, associated with flow disturbances in the corona, are much larger than capillary effects [16]. The pressure associated with the inertial effects can be estimated as $p_{\text{inert}} \sim \rho u_r^2$. The pressure associated with surface tension is estimated using the Young-Laplace equation $p_\sigma \sim \sigma \, \partial h / \partial r^2 \sim \sigma h_{\text{lam}} / R_{\text{corona}}^2$. The condition for splash, $p_{\text{inert}} \gg p_\sigma$, with the help of Eqs. (7) and (9) can be expressed in the form

$$\frac{D_0 \text{We}}{h_{\text{lam}}(t)} \gg 1, \tag{11}$$
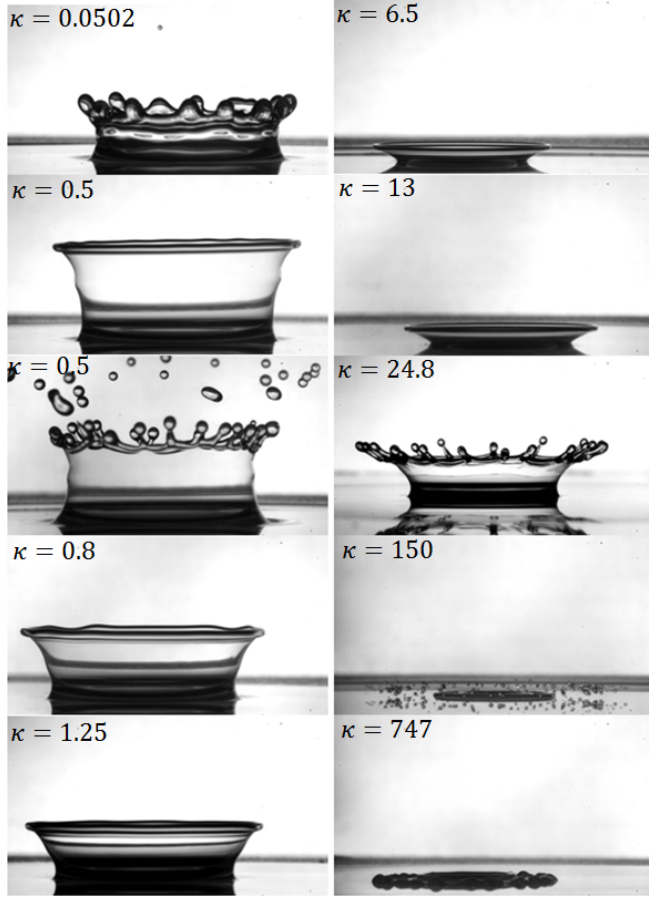
valid for long times, $t \gg \tau D_0 / U_0$.

FIG. 9. Effect of viscosity ratio (κ) on the outcome of drop impact with $\delta = 0.25$, $D_0 = 2$ mm, and $U_0 = 2.3$ m/s.

The thickness of the lamella $h_{\mathrm{lam}}(t)$ reduces with time. The instant at which splash occurs can be estimated from Eqs. (11) and (8) as $t_{\mathrm{splash}} \sim D_0/U_0$. The corresponding lamella thickness is $h_{\mathrm{splash}} \sim D_0 \mathrm{We}^{-1}$.

On the other hand, at larger times the boundary-layer thickness becomes comparable with the lamella thickness. At these times, the inviscid solution (8) is no longer valid. The flow is damped by viscosity and the velocity field vanishes. This situation leads to the appearance of a nearly stationary residual wall film.

The similarity solution for the expansion of the viscous boundary layer has been obtained in Ref. [38] for the case of drop impact onto a dry smooth substrate. It is obvious that the same analysis can be applied to the case of drop impact onto a wall layer of the same liquid, since it is immaterial whether the fluid exists on the wall before impact or arrives with the drop, a boundary layer still develops. The thickness of the lamella, determined in Eq. (8) for large times, is scaled as $h_{\mathrm{lam}} \sim D_0^3 U_0^{-2} t^{-2}$, while the thickness of the viscous boundary layer scales as $h_{\mathrm{visc}} \sim \sqrt{\nu t}$. Therefore, the time at which the viscous boundary layer reaches the free surface of the lamella, $h_{\mathrm{lam}} = h_{\mathrm{visc}}$, can be estimated as $t_{\mathrm{visc}} \sim D_0/U_0 \mathrm{Re}^{1/5}$. The thickness of the wall film at this instant is correspondingly $h_{\mathrm{visc}} \sim D_0 \mathrm{Re}^{-2/5}$. In the experimental study [39], this scaling has been successfully confirmed. The measured and computed residual film thickness at the bottom of the crater is proportional to h_{visc} and depends also on the relative initial thickness of the wall film.

(a) formation of a crater and viscous boundary layer

(b) viscous boundary layer in a drop region

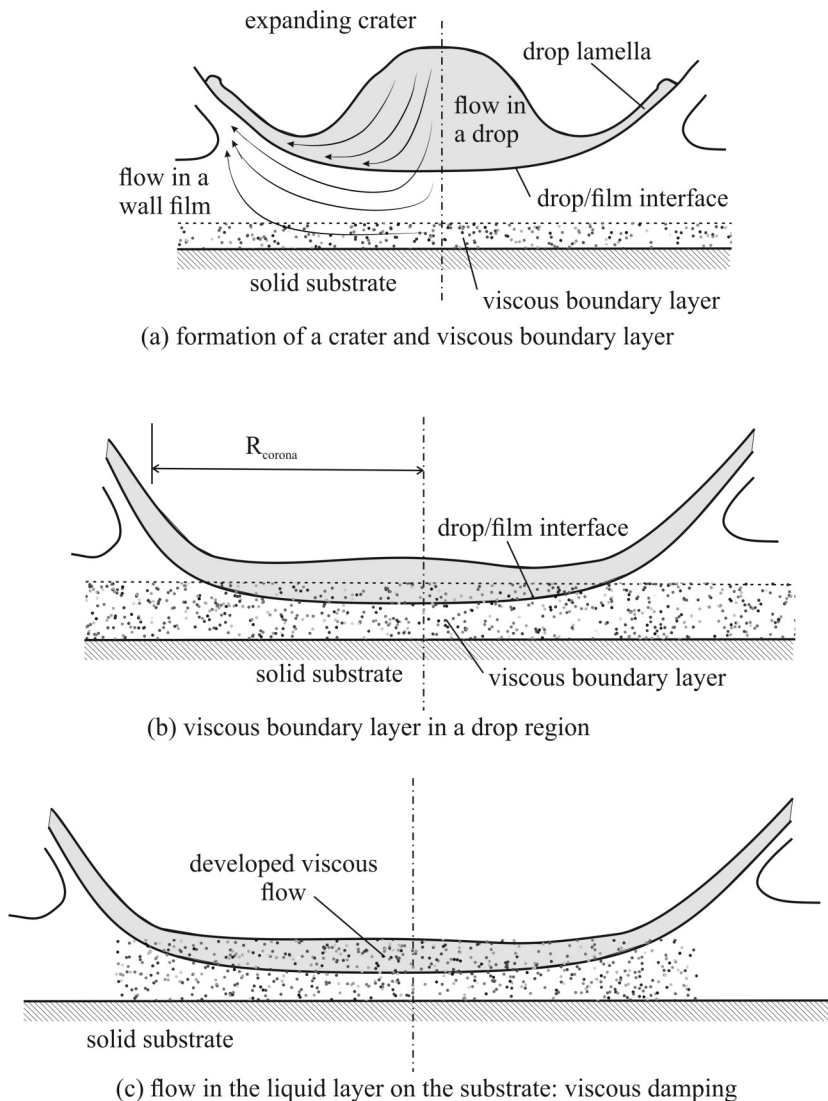(c) flow in the liquid layer on the substrate: viscous damping

FIG. 10. Consecutive stages of drop impact onto a wetted substrate: (a) initial drop deformation and penetration into the wall film, inception of the viscous boundary layer on the wall; (b) boundary-layer growth leads to intersection with the drop/film liquid interface; and (c) liquid layer in the crater is thinner than the viscous boundary layer.

An impacting drop splashes when the residual lamella thickness, which is scaled well by h_{visc}, is smaller than the critical lamella thickness h_{splash}. It can be shown that the threshold condition $h_{\mathrm{visc}} = h_{\mathrm{splash}}$ leads to

$$\mathrm{We}\mathrm{Re}^{2/5} \gg 1. \tag{12}$$

This condition is very close to the widely used threshold criterion $K > K_{\mathrm{splash}}$, which allows us to assume that our description of the mechanisms of splash accounts for the main physical factors.

C. Evolution of the drop/liquid interface at large times: Drop and film liquids are the same

At large times, the flow in the spreading lamella includes two layers, that of the drop and that of the film. The velocity field is described using the similarity solution [38]

$$u_r = \frac{r}{t} f'\left[\frac{z}{\sqrt{\nu t}}\right], \quad u_z = -\frac{2\sqrt{\nu}}{\sqrt{t}} f\left[\frac{z}{\sqrt{\nu t}}\right], \tag{13}$$

where $\xi \equiv z/\sqrt{\nu t}$ is the similarity variable.

The velocity field satisfies the continuity equation. The dimensionless function $f(\xi)$ is obtained from the momentum balance equation [38] and has to satisfy the boundary conditions

$$f(0) = 0, \quad f'(0) = 0, \quad \lim_{\xi \to \infty} f'(\xi) = 1. \tag{14}$$

It has been shown in Sec. IV B that the height h_i of a liquid interface at long times approaches a residual thickness, which is scaled as $h_i = \chi(\delta) D_0 \mathrm{Re}^{-2/5}$, where $\chi(\delta)$ is a dimensionless constant. This conclusion is valid also for the drop/liquid interface. The constant χ is determined by the relative initial film thickness δ. The value of ξ corresponding to the height $z = h_i$ is small at large times. Therefore, the velocity profile can be linearized, $f(\xi) \approx B\xi^2/2$, where $B = f''(0)$. Correspondingly, the velocity and the shear stress at the drop/film interface are

$$u_{ri} = \frac{B\chi D_0^{3/5} r}{\nu^{1/10} t^{3/2} U_0^{2/5}}, \quad \tau_i = \frac{B\rho\sqrt{\nu} r}{t^{3/2}}, \quad \text{at} \quad z = \chi \frac{D_0^{3/5} \nu^{2/5}}{U_0^{2/5}}. \tag{15}$$

In the case when the liquids of the drop and of the wall film are the same, the velocity and the shear stress near the drop/film interface are smooth, continuous functions.

V. SPLASHING THRESHOLD: DROP AND FILM OF DIFFERENT LIQUIDS

When the drop and wall film are different liquids, the similarity solution described in Sec. IV A is not valid for larger times, when the thickness of the viscous boundary layer is of the same order as the height of the drop/film interface.

A. Viscosity of the film is much larger or much smaller than the viscosity of the drop liquid

If the viscosity of the drop is much larger that the viscosity of the wall film, the time t_{visc} is determined mainly by the time the viscous boundary-layer takes to propagate into the film region. In this case, it is possible to assume that the splashing threshold is determined mainly by the properties of the wall film liquid. The limiting case of such a situation is an impact of a solid particle onto a wetted wall.

Analogously, if the viscosity of the wall film is much larger than the viscosity of the drop, the time for the viscous boundary-layer expansion in the film layer is much shorter than the time of boundary-layer expansion in the drop. In this case, we can assume that the splashing threshold is determined mainly by the drop properties.

It is therefore prudent to define two dimensionless K numbers

$$K_{\mathrm{d}} = \mathrm{We}_{\mathrm{d}}^{1/2} \mathrm{Re}_{\mathrm{d}}^{1/4}, \quad K_{\mathrm{f}} = \mathrm{We}_{\mathrm{f}}^{1/2} \mathrm{Re}_{\mathrm{f}}^{1/4}, \tag{16}$$

where the subscripts d and f denote the use of the drop or wall film liquid properties respectively.

The experimentally obtained outcome map for drop impact is shown in Fig. 11 for the range of the dimensionless thickness of the initial wall film $0.036 < \delta < 0.29$ and for the range of the viscosity ratio $10^{-4} < \kappa < 10^4$. Two splashing regions can be clearly identified. Region I, defined by $K_{\mathrm{d}} < 80$ and $K_{\mathrm{f}} > 155$, corresponds to the case when the viscosity of the drop is much higher than the viscosity of the film. The splashed liquid consists mainly of liquid from the wall film.
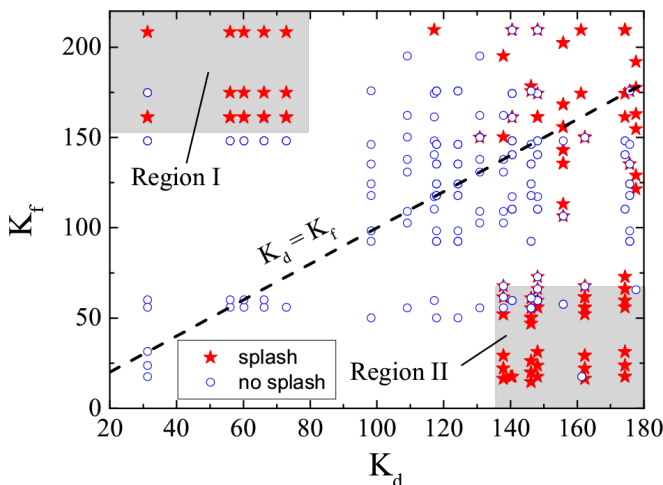
FIG. 11. Map of the experimentally observed outcomes of drop impact. Region I of splash occurrences corresponds to very viscous drops, and region II corresponds to splash occurrences on a very viscous wall film. The relative film thickness varies in the range $0.036 < \delta < 0.29$ and the viscosity ratio in the range $10^{-4} < \kappa < 10^4$.

Region II, associated with $K_d > 135$ and $K_f < 70$, corresponds to conditions when the wall film viscosity is much larger than the drop viscosity. Then the splashed liquid consists of liquid from the drop.

When the viscosity of the drop and the wall film liquids are of the same order of magnitude, the splash cannot be described by K_d and/or K_f separately. Further analysis is required for this range of parameters, which is designated region III in Fig. 11.

B. The properties of both liquids are of the same order of magnitude, $\kappa \approx 1$

Consider a similarity solution for the flow in the drop and in the wall film at large times. The type of this similarity is the same as described in Sec. IV B. The solution has to satisfy the continuity of the radial velocity and of the shear stress at the drop/film interface. This condition can be written with the help of Eq. (15):

$$\frac{B_d \chi_d}{\nu_d^{1/10}} = \frac{B_f \chi_f}{\nu_f^{1/10}}, \quad B_d \rho_d \sqrt{\nu_d} = B_f \rho_f \sqrt{\nu_f}, \tag{17}$$

where B_d and χ_d are dimensionless constants determining the solution in the drop layer, while B_f and χ_f determine the solution in the wall film layer.

The roots of the system of linear equations (17) are

$$\chi_d = \chi_f \frac{\rho_d \nu_d^{3/5}}{\rho_f \nu_f^{3/5}}, \quad B_f = B_d \frac{\rho_d \nu_d^{1/2}}{\rho_f \nu_f^{1/2}}. \tag{18}$$

The constant positive displacement Δ of the velocity field in the drop layer in the axial direction due to the difference in viscosity in the film can be found using the expression for h_i from (15) and the expression for χ_d from (18)

$$\Delta = \chi_f \frac{D_0^{3/5} \nu_f^{2/5}}{U_0^{2/5}} - \chi_d \frac{D_0^{3/5} \nu_d^{2/5}}{U_0^{2/5}} = \chi_f \frac{D_0^{3/5} (\mu_f - \mu_d)}{U_0^{2/5} \rho_f \nu_f^{3/5}}. \tag{19}$$
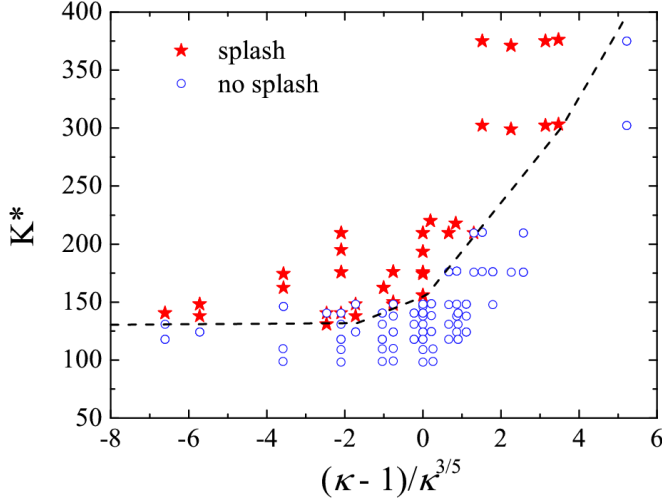
FIG. 12. Map of the experimentally observed outcomes of drop impact for region III, when the viscosities of the drop and wall film liquids are comparable and $K_d > 100$ and $K_f > 100$. The relative initial wall film thickness varies in the range $0.05 < \delta < 0.22$. The data belonging to regions I and II (determined from Fig. 11) are not included.

It can be shown that the residual film thickness is determined by the dimensionless parameter $\Delta/(D_0 \mathrm{Re}_d^{-2/5})$, associated with the difference of the liquid viscosities.

In the case when the densities of the liquids are comparable, the dimensionless parameter can be reduced to

$$\frac{\Delta}{D_0 \mathrm{Re}_d^{-2/5}} \sim \frac{\kappa - 1}{\kappa^{3/5}}. \tag{20}$$

Next, since the viscosities of two liquids are comparable, the flow in the corona consists of both liquids. The capillary pressures in the film and in the drop liquids are determined using the Young-Laplace equations: $p_{\sigma d} \approx \sigma_d h / R_{\mathrm{corona}}^2$ and $p_{\sigma f} \approx \sigma_f h / R_{\mathrm{corona}}^2$, respectively. The splash therefore occurs first in the region with smaller surface tension. Following this assumption, the effective splashing parameter can be defined:

$$K^* = \mathrm{Re}_d^{1/4} \mathrm{We}^{*1/2}, \quad \mathrm{We}^* = \frac{(\rho_f + \rho_d) D_0 U_0^2}{2 \min\{\sigma_d; \sigma_f\}}. \tag{21}$$

It should be noted that the flow in a spreading drop is influenced also by the interfacial tension σ_{df}. The value of σ_{df} and the pressure difference $p_{\sigma d} - p_{\sigma f}$ determine the curvature of the drop/film interface near any triple point common to two liquids and gas. Following this assumption, the effect of the interfacial tension σ_{df} on the splashing threshold is negligibly small and is not considered in this study.

Since the densities of all the liquids in the experiments are comparable, it is not possible at this stage to identify experimentally the influence that a density difference may have on the impact. Therefore, in the present case, simply an average density is used for computing the Weber number We^* in Eq. (21).

The map of the drop impact outcomes shown in Fig. 12 is based on experimental data for impacts of drops onto a wall film with comparable viscosity. The range of the relative initial wall film thickness is $0.05 < \delta < 0.22$. This range is chosen, since for the same drop and wall film liquids the threshold value of the K number depends in this range only very weakly on δ [24]. The data belonging to regions I and II (determined from Fig. 11) are excluded from the graph. It is evident

from this map that the splashing threshold is determined by the dependence of the critical number K^* on the viscosity ratio parameter $(\kappa - 1)/\kappa^{3/5}$.

VI. CONCLUSION

In this study, the single drop impact onto a thin liquid wall film of a different liquid is investigated. The viscosities of the drop and wall film are varied widely, leading to viscosity ratios in the range $10^{-4} < \kappa < 10^4$. Three regions of splash are identified. In region I (associated with the case $\kappa \ll 1$), the splash is determined by the K_f number based on the properties of the wall film. In region II (associated with the case $\kappa \gg 1$), the splash is determined by the K_d number based on the properties of the drop liquid. In region III, a scaling is proposed based on the assumption that splash is initiated in the liquid layer with smaller surface tension. The threshold K^* number is a function of the dimensionless term $(\kappa - 1)/\kappa^{3/5}$. These results are of a predictive nature.

ACKNOWLEDGMENT

---

[1] A. L. Yarin, Drop impact dynamics: Splashing, spreading, receding, bouncing, Annu. Rev. Fluid Mech. **38**, 159 (2006).

[2] C. Josserand and S. T. Thoroddsen, Drop impact on a solid surface, Annu. Rev. Fluid Mech. **48**, 365 (2016).

[3] M. Pasandideh-Fard, V. Pershin, S. Chandra, and J. Mostaghimi, Splat shapes in a thermal spray coating process: Simulations and experiments, J. Thermal Spray Tech. **11**, 206 (2002).

[4] S. T. Thoroddsen, T. G. Etoh, and K. Takehara, High-speed imaging of drops and bubbles, Annu. Rev. Fluid Mech. **40**, 257 (2008).

[5] A. L. Yarin, I. V. Roisman, and C. Tropea, *Collision Phenomena in Liquids and Solids* (Cambridge University Press, Cambridge, UK, 2017).

[6] S. Gouin, Microencapsulation: Industrial appraisal of existing technologies and trends, Trends Food Sci. Technol. **15**, 330 (2004).

[7] B. F. Gibbs, S. Kermasha, I. Alli, and C. N. Mulligan, Encapsulation in the food industry: A review, Int. J. Food Sci. Nutr. **50**, 213 (1999).

[8] J. Kim, Spray cooling heat transfer: The state of the art, I. J. Heat Fluid Flow **28**, 753 (2007).

[9] G. Liang and I. Mudawar, Review of mass and momentum interactions during drop impact on a liquid film, Int. J. Heat Mass Transf. **101**, 577 (2016).

[10] D. W. Stanton and C. J. Rutland, Multi-dimensional modeling of thin liquid films and spray-wall interactions resulting from impinging sprays, Int. J. Heat Mass Transf. **41**, 3037 (1998).

[11] L. Andreassi, S. Ubertini, and L. Allocca, Experimental and numerical analysis of high pressure diesel spray-wall interaction, Int. J. Multiph. Flow **33**, 742 (2007).

[12] R. Rioboo, C. Tropea, and M. Marengo, Outcomes from a drop impact on solid surfaces, Atomiz. Spray **11**, 12 (2001).

[13] I. V. Roisman, K. Horvat, and C. Tropea, Spray impact: Rim transverse instability initiating fingering and splash, and description of a secondary spray, Phys. Fluids **18**, 102104 (2006).

[14] S. K. Alghoul, C. N. Eastwick, and D. B. Hann, Normal droplet impact on horizontal moving films: An investigation of impact behavior and regimes, Exp. Fluids **50**, 1305 (2011).

[15] K.-L. Pan, K.-R. Cheng, P.-C. Chou, and C.-H. Wang, Collision dynamics of high-speed droplets upon layers of variable thickness, Exp. Fluids **45**, 435 (2008).

[16] A. L. Yarin and D. A. Weiss, Impact of drops on solid surfaces: Self-similar capillary waves, and splashing as a new type of kinematic discontinuity, J. Fluid Mech. **283**, 141 (1995).

[17] I. V. Roisman and C. Tropea, Impact of a drop onto a wetted wall: Description of crown formation and propagation, J. Fluid Mech. **472**, 373 (2002).

[18] I. V. Roisman, N. P. van Hinsberg, and C. Tropea, Propagation of a kinematic instability in a liquid layer: Capillary and gravity effects, Phys. Rev. E **77**, 046305 (2008).

[19] E. Berberović, N. P. van Hinsberg, S. Jakirlić, I. V. Roisman, and C. Tropea, Drop impact onto a liquid layer of finite thickness: Dynamics of the cavity evolution, Phys. Rev. E **79**, 036306 (2009).

[20] G. Taylor, The dynamics of thin sheets of fluid. III. Disintegration of fluid sheets, Proc. R. Soc. London, Ser. A **253**, 313 (1959).

[21] I. V. Roisman, On the instability of a free viscous rim, J. Fluid Mech. **661**, 206 (2010).

[22] C. Mundo, M. Sommerfeld, and C. Tropea, Droplet-wall collisions: Experimental studies of the deformation and breakup process, Int. J. Multiph. Flow **21**, 151 (1995).

[23] G. E. Cossali, A. Coghe, and M. Marengo, The impact of a single drop on a wetted solid surface, Exp. Fluids **22**, 463 (1997).

[24] R. Rioboo, C. Bauthier, J. Conti, M. Voue, and J. De Coninck, Experimental investigation of splash and crown formation during single drop impact on wetted surfaces, Exp. Fluids **35**, 648 (2003).

[25] I. V. Roisman, A. Lembach, and C. Tropea, Drop splashing induced by target roughness and porosity: The size plays no role, Adv. Colloid Interface Sci. **222**, 615 (2015).

[26] R. L. Vander Wal, G. M. Berger, and S. D. Mozes, The splash/non-splash boundary upon a dry surface and thin fluid film, Exp. Fluids **40**, 53 (2006).

[27] T. Okawa, T. Shiraishi, and T. Mori, Effect of impingement angle on the outcome of single water drop impact onto a plane water surface, Exp. Fluids **44**, 331 (2008).

[28] A. Geppert, D. Chatzianagnostou, C. Meister, H. Gomaa, G. Lamanna, and B. Weigand, Classification of impact morphology and splashing/deposition limit for n-hexadecane, Atomiz. Spray **26**, 983 (2016).

[29] N. Chen, H. Chen, and A. Amirfazli, Drop impact onto a thin film: Miscibility effect, Phys. Fluids **29**, 092106 (2017).

[30] A. Geppert, A. Terzis, G. Lamanna, M. Marengo, and B. Weigand, A benchmark study for the crown-type splashing dynamics of one- and two-component droplet wall–film interactions, Exp. Fluids **58**, 172 (2017).

[31] Z. Jian, Drop impact on solid: Splashing transition and effect of the surrounding gas, Ph.D. thesis, Université Pierre et Marie Curie-Paris VI, France, 2014.

[32] H. M. Kittel, I. V. Roisman, and C. Tropea, Outcome of drop impact onto a liquid film of different viscosities, in *ILASS-Europe 2016, 27th Annual Conference on Liquid Atomization and Spray Systems* (Brighton, UK, 2016).

[33] A. I. Fedorchenko and A.-B. Wang, On some common features of drop impact on liquid surfaces, Phys. Fluids **16**, 1349 (2004).

[34] See Supplemental Material at http://link.aps.org/supplemental/10.1103/PhysRevFluids.3.073601 for several movies of drop impact onto a thin film.

[35] S. Bakshi, I. V. Roisman, and C. Tropea, Investigations on the impact of a drop onto a small spherical target, Phys. Fluids **19**, 032102 (2007).

[36] A. Bisighini, G. E. Cossali, C. Tropea, and I. V. Roisman, Crater evolution after the impact of a drop onto a semi-infinite liquid target, Phys. Rev. E **82**, 036319 (2010).

[37] I. V. Roisman, E. Berberović, and C. Tropea, Inertia dominated drop collisions. I. On the universal flow in the lamella, Phys. Fluids **21**, 052103 (2009).

[38] I. V. Roisman, Inertia dominated drop collisions. II. An analytical solution of the Navier-Stokes equations for a spreading viscous film, Phys. Fluids **21**, 052104 (2009).

[39] N. P. Van Hinsberg, M. Budakli, S. Göhler, E. Berberović, I. V Roisman, T. Gambaryan-Roisman, C. Tropea, and P. Stephan, Dynamics of the cavity and the surface film for impingements of single drops on liquid films of various thicknesses, J. Colloid Interface Sci. **350**, 336 (2010).